Active Flutter Suppression—A Flight Test Demonstration

Kenneth L. Roger* and Garold E. Hodges†
The Boeing Company, Wichita, Kansas

and

Larry Felt‡
Wright Patterson Air Force Base, Ohio

The first flight test demonstration of active flutter suppression has been successfully completed. The Control Configured Vehicles (CCV) B-52 test airplane was twice flown 10 knots faster than its flutter speed relying solely on an automatic control system for adequate damping. The design, safety considerations, mechanization, ground testing, and flight testing of the flutter mode control system are reported. Comparisons between flight test and theoretical results are presented. The system was tested at heavy and light airplane weights and tested for compatibility with simultaneous ride control, maneuver load control, fatigue reduction, and augmented stability.

Introduction

MODERN high-performance aircraft are designed for maximum aerodynamic efficiency with minimum structural weight. The resulting airframe flexibility often leads to aeroelastic instabilities, such as flutter. Currently, passive methods are used to solve the flutter problem, e.g., additional stiffness, mass balancing, or speed restrictions. These passive methods result in significant performance penalties.

During the past several years, many programs have investigated active methods of altering or controlling airframe flexibility with flight controls. Flight tests of the B-52 and XB-70 aircraft more than seven years ago successfully demonstrated the concept of using flight controls to alter aircraft structural dynamic characteristics. More recently, several active control concepts have been analytically applied to a wide variety of aircraft, including the SST, C-5A, 747, B-1, F-4, YF-16, and the Advanced Technology Transport. Some of these programs have included active control aeroelastic wind tunnels models to verify design predictions and to supplement analyses. This expanding experience and technology base in flight control and in flutter prediction techniques has led to the application of active control methods to solve flutter problems with smaller performance penalties. The evolution of CCV technology from an idea to a B-52 flight demonstration and eventually to the design of a prototype fighter airplane, the YF-16, is discussed in Ref. 1.

The Wichita Division of The Boeing Company, under the sponsorship of the Air Force Flight Dynamics Laboratory, is conducting a B-52 Control Configured Vehicles (CCV) program to demonstrate the benefits of applying advanced flight control technology to a large flexible airplane. This program was initiated in July 1971 and was completed in June 1974.

One of the CCV systems demonstrated during this program was the Flutter Mode control (FMC). This system uses active aileron and flaperon control surfaces to stabilize a 2.4 Hz symmetric wing flutter problem. The synthesis, analysis, and implementation studies of the FMC system is discussed in Ref. 2.

On Aug. 2, 1973 aviation history was made in the skies over western Kansas when the CCV B-52 test aircraft was flown 10 knots faster than its flutter speed. This was the first time an aircraft had been flight tested above its flutter speed relying solely on an active flutter control system to augment the structural damping. The flight was a significant step in the acceptance and incorporation of this new technology into future aircraft designs. The paper will report the details of this series of flight test demonstrations and summarize the system design.

B-52 CCV Program

Four new CCV systems were designed for flight demonstration on the Air Force flight research airplane, NB-52E, AF56-632, which was previously used during the LAMS program.[3] This aircraft is highly instrumented for inflight testing.

The four CCV concepts developed under this program were Ride Control (RC), Flutter Mode Control (FMC), Maneuver Load Control (MLC), and Augmented Stability (AS). The LAMS system was modified to be compatible with the other CCV systems and is denoted as the Fatigue Reduction (FR) system. All systems were implemented using off-the-shelf hardware and, except for FMC, general purpose analog computers. The systems were designed to meet performance objectives with each system operating individually and with all CCV concepts operating simultaneously.

The primary goal of the Flutter Mode Control system was to analytically extend the flutter placard speed (V_p) 30% and flight demonstrate the system 10 knots above the flutter speed. Compatibility with other systems was to be demonstrated up to within a few knots of the unaugmented flutter speed.

The Ride Control system tested early in the program demonstrated a 30% reduction in vertical acceleration response and a 44% reduction in lateral acceleration response to turbulence at the crew station: these reductions met the established program goal of 30% reduction. The Ride Control system synthesis, design, and analysis is presented in Ref. 4 and flight test results in Ref. 5.

The Maneuver Load Control system was designed to produce a 10% reduction in design wing root bending moment

Presented as Paper 74-402 at the AIAA/ASME/SAE 15th Structures, Structural Dynamics and Materials Conference, Las Vegas, Nevada, April 17-19, 1974; submitted April 12, 1974; revision received December 16, 1974. This work was sponsored by the Air Force Dynamics Laboratory under Contract F33615-71-C-1926.

Index categories: Aeroelasticity and Hydroelasticity; Aircraft Handling; Stability, and Control; Aircraft Testing (Including Component Wind Tunnel Testing).

*Senior Specialist Structural Dynamics. Member AIAA.
†Senior Specialist Control Dynamics. Member AIAA.
‡Aerospace Engineer, Air Force Flight Dynamics Laboratory. Member AIAA.

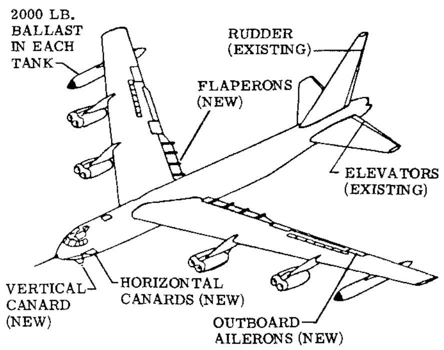

SURFACES	CCV CONCEPTS				
	RCS	FMC	MLC	AS	FR
RUDDER				X	
ELEVATOR			X	X	X
FLAPERON		1 SEGMENT	X		
OUTBOARD AILERON		X	X		X
HORIZONTAL CANARD	X				
VERTICAL CANARD	X				

Fig. 1 B-52 CCV control surfaces.

at the flight condition that produces maximum wing root maneuver load. The Augmented Stability system was designed to provide required stability and flying qualities for an aircraft configuration not meeting inherent stability requirements for Dutch roll and short period pitch. The Fatigue Reduction System was designed to reduce fatigue damage rates due to turbulence at critical wing and fuselage locations. Operational and performance compatibility among all systems was demonstrated during the latter part of the test program.

Analytical studies were conducted to determine surface placement and size for each CCV concept and to evaluate the potential of various configurations to meet performance objectives. Existing B-52 control surfaces used for CCV functions are elevators and rudder. New additional surfaces consist of three-segment flaperons, outboard ailerons, horizontal, and a vertical canard. In Fig. 1, the surface arrangement and usage for each concept is shown. The three segment flaperon replaced the existing inboard flaps.

FMC System Design

Configuration Selection

A flutter mode within the speed capabilities of the B-52 test airplane was created by adverse ballasting of the wing drop tanks. The left and right tanks, which normally carry 19,500 lbs of fuel each, were modified to carry, instead, 2000 lbs of lead in the forward end of each tank. The lead weights were enclosed in steel and attached as shown in Fig. 1. Because of the light weight of the ballast, compared with the normal fuel load, only local modifications to the drop tanks were required. The capability to jettison the drop tanks was retained.

At the 21,000 ft test alt, the ballasted airplane was predicted to flutter at 315 knots (calibrated airspeed) with a full wing, and at 330 knots with a half-full wing—both speeds well under the normal level flight limit of 400 knots. The flutter mode in each case was predicted to be symmetric, about 2.4 Hz, and mild. The rate of loss of damping was expected to be about 0.01 g per 10 knots.

The flutter mode consisted of wing 2nd vertical bending, wing 1st torsion, wing 1st fore and aft bending, outboard engine strut side bending, and body nose and tail vertical bending. Flutter does not occur if the drop tanks are either full or empty, or if the outboard wing fuel tank is empty. Analytically the flutter is most severe when the ballast is 2,000 lb (as chosen) and as far ahead of and below the wing as possible.

The characteristics of the flutter mode were important in planning the entire CCV program: a) Its mildness made testing 10 knots above flutter with a dual FMC system feasible. b) Its low frequency permitted the use of a linear, yet relatively low cost control system. c) Its existence within the bandpass of the Ride Control and Fatigue Reduction systems provided a test of the adequacy of their design criteria.

Design Methods

One of the purposes of the program was to see whether existing analytical methods were adequate for predicting the performance of the new control systems. The analytical tools were conventional, except perhaps in the scope of their application. The structural generalized coordinates were selected by vibration analysis, retaining the 27 lowest frequency symmetric modes (see Table 1 for those under 5 Hz) and, when applicable, the 27 lowest frequency antisymmetric modes.

Unsteady aerodynamic forces acting on the airplane were represented by the doublet lattice method, with the airplane paneled as shown in Fig. 2. The wing, engines, body nose, tail, and control surfaces were aerodynamically coupled with each other.

The interfacing of the point frequency unsteady aerodynamic coefficients with Laplace transform equations of motion was done with the use of approximating functions. Figure 3 shows a typical aerodynamic coefficient plotted as s

Table 1 Low frequency symmetric vibration modes

Mode	Frequency (260,000 lbs)	Frequency (375,000 lbs)
Wing	0.88 Hz	0.78 Hz
Wing	1.74	1.68
Inboard engine	2.01	2.00
Outboard engine	2.15	2.13
Wing and body	2.41[a]	2.22[a]
Inboard engines and body	2.97	2.78
Inboard engines and body	3.14	3.11
Wing and outboard engines	3.77	3.46

[a]Dominant mode during flutter.

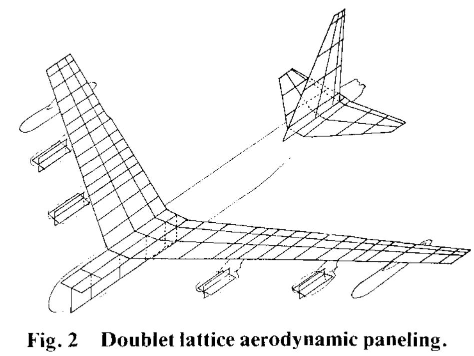

Fig. 2 Doublet lattice aerodynamic paneling.

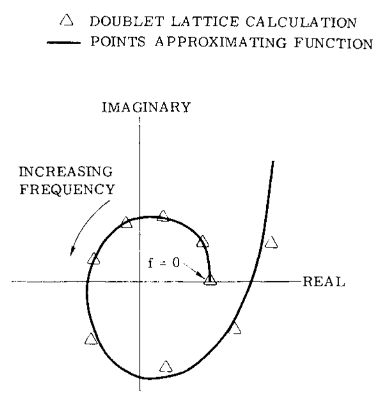

Fig. 3 Aerodynamic coefficient approximating function.

moves up the imaginary axis, and the "best fit" approximating function. The approximating function chosen was a rational polynomial with denominator roots on the left real axis. It can be considered to be a physically realizable frequency interpolating function for the unsteady aerodynamic coefficients. A function was found for each element in the aerodynamic influence matrix. The resulting functions were generalized and included as part of the equations of motion, raising the order of the differential equations once for each denominator root. Two roots (4th-order equation) were usually used, with four roots (6th-order equations) for accuracy checks and one root (3rd-order equations) for the hybrid computer. Because of the continuous nature of the approximating functions the equations of motion were expected to be valid in the region of the s-plane near the imaginary axis (low positive and negative damping) throughout the frequency range analyzed.

Synthesis Constraints

Synthesis constraints were imposed on the system to assure that adequate performance would be provided with variations from that predicted by the nominal mathematical model. These constraints provided a tolerance for variations in surface effectiveness, airplane modeling accuracy, and system hardware. Each of the following constraints was evaluated independently with all other parameters held at nominal values: a) The system will remain stable with feedback sensor location variations ± 60 in. parallel to the local elastic axis. b) Stability margins will be greater than ± 6 db gain margin at nominal phase and greater than ± 60° phase margin at nominal gain at frequencies below 3 Hz. The phase margin will increase linearly to ± 180° at nominal gain for structural modes above 5 Hz. c) The FMC system will remain stable in atmospheric turbulence of the same intensity used for structural design. d) Implementation will provide a single-fail operate capability. e) Sustained residual acceleration oscillations in still air at the pilot's station will be no greater than 0.014 g peak-to-peak. (This acceleration amplitude is less than the human perceptible level.)

System Synthesis

Root locus linear analysis techniques using equations of motion with from 18 to 27 structural modes were used to synthesize the FMC system. The large set of high-order equations of motion dictated that the studies be conducted with as many as 200 roots. The required eigenvalue solutions were done using the Q-R real matrix algorithm and 16-digit numerical accuracy. A hybrid computer simulation including only six structural modes provided the analytical method for evaluating the system nonlinear effects. FMC system nonlinearities evaluated included backlash in the actuator attachments, servovalve threshold, control surface displacement limits, and surface rate saturation. Power spectral density analyses were conducted to assess the effect of the FMC on gust loads at critical structural locations and to determine surface displacement and rate requirements. A fixed-base pilot simulation was used to evaluate the flying qualities.

The FMC is composed of two independent control loops, sensors to surfaces: the outboard aileron loop and the outboard flaperon. Each loop sufficiently augments the damping to meet system performances objectives. Various combinations of sensor types and placement and control surface placement were evaluated at critical flight conditions using root locus techniques to determine the damping improvement and coupling with other structural modes. The selected configuration was then evaluated at all flight conditions.

The FMC system senses wing vertical acceleration near the external tanks, which is passed through a shaping filter and used to drive the outboard ailerons. A second sensor measures wing vertical acceleration between the engine pods. This signal is shaped and used to drive the outboard flaperon. Figure 4 depicts the FMC sensor and surface locations used

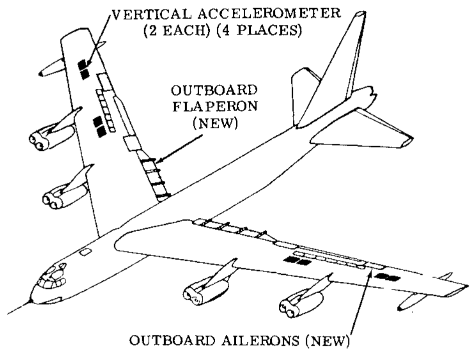

Fig. 4 FMC control surface and sensor locations.

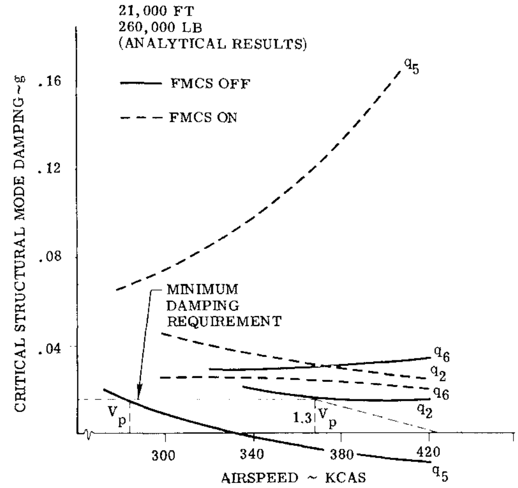

Fig. 5 FMC functional block diagram.

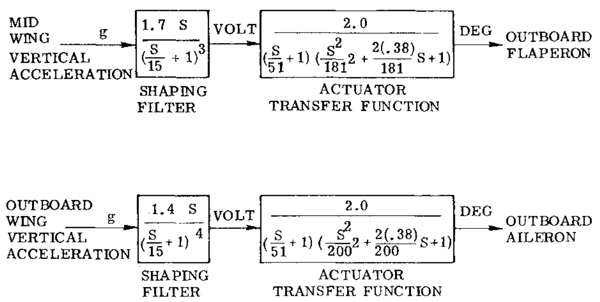

Fig. 6 FMC predicted flutter speed improvement.

for the B-52 airplane. A functional block diagram of the FMC system and associated actuator is illustrated in Fig. 5.

The FMC system was predicted to increase flutter placard speed more than 30% as illustrated in Fig. 6, for the mid weight wing (260,000 lb gross weight). The effect of FMC on other significant structural modes (q_2 and q_6) are also shown. Figure 7 shows that the FMC exceeds the goal of 30% increase in Vp with the model tolerances previously discussed. Gain margin is greater than ± 14db and the phase margin exceeds ± 120° for each control surface.

FMC compatibility was evaluated with other CCV systems and critical airplane parameters. The 30% improvement in flutter placard speed was achieved with all CCV systems operating simultaneously. The increase in gust loads at all critical wing and body locations was less than 3%.

Flight Safety Considerations

Flight safety was included as an integral part of the FMC synthesis and implementation. Independent sensor, electronics, control surfaces, and secondary power was used for each feedback loop to provide redundancy.

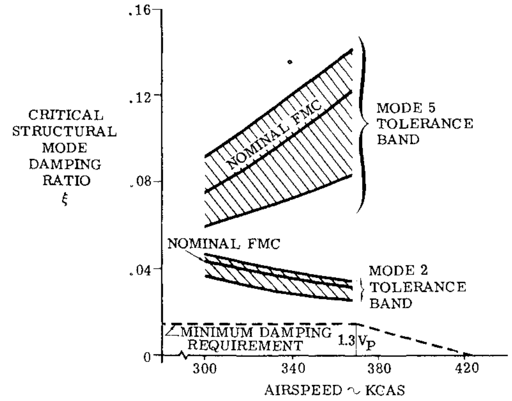

Fig. 7 Tolerance effect on flutter.

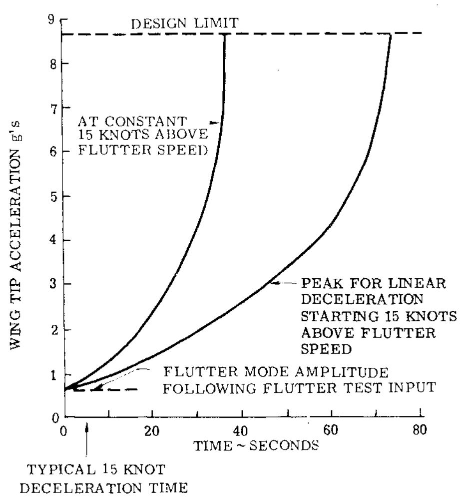

Fig. 8 Wing tip acceleration after total FMC disengage.

A safety monitor detects differences in the two outboard aileron channels and will shut off this system if channel differences exceed 5°. The flaperon safety monitor performs the same function in a similar manner for the flaperon system. The disengage levels of the monitors were selected to be as large as possible without causing acceleration and moments to approach design limits.

Another safety feature was to hardwire the FMC system to increase reliability (Each of the other CCV systems was wired on the on-board analog computers). Since the flutter mode is a mild and only 2.4 Hz, the pilot has adequate time to reduce airspeed before structural failure should a total loss of the FMC function occur. Piloted simulator results show that approximately five seconds are required for the pilot to react and decelerate the airplane 15 knots from speeds above the flutter speed, using airbrakes and throttle. The 5 sec deceleration interval is much less than the time necessary for the flutter mode to diverge to structural failure. Figure 8 illustrates the time to reach wing design load factor following total FMC disengage during a strong flutter test input.

Telemetry of selected channels of data provided real-time monitoring of the structural activity at selected locations on the test vehicle. Parameters monitored by telemetry included control surface deflections and double integrated acceleration response at the left wing tip (vertical and longitudinal), right wing tip (vertical), body nose (vertical), aft body (lateral), horizontal tail tip (vertical), and fin tip (lateral). Flutter testing was conducted using pilot inputs sequentially to the elevator, rudder, and inboard ailerons/spoilers.

FMC Mechanization

The new equipment consists of hydraulic actuators, outboard aileron surfaces, flaperon surfaces, wing mounted accelerometers, special control panels at the pilot and flight engineer's station, signal shaping electronics and ballasted wing tip tanks. The aileron and flaperon control surfaces were actuated independently.Each surface had chord and spanwise dimensions as given in Table 2.

A photograph of the test airplane with the CCV control surfaces installed is presented in Fig. 9. The aileron surfaces are mass balanced and partially aerodynamically balanced. The flaperon surfaces were not mass balanced since analysis showed the surfaces to be flutter free at the test speeds, and were not aerodynamically balanced.

High-performance electrohydraulic actuators are used to drive each FMC control surface. Two critical actuation parameters are backlash and bandwidth. Since the flutter mode becomes unstable as the FMC gain is reduced, a limit cycle is produced for signal amplitudes less than the backlash. Total actuator backlash was designed and verified by tests to be less than 0.175°. The corresponding acceleration at the pilot's station is less than 0.014 *g* peak-to-peak, which is less than the perceptible level. No limit cycle acceleration was perceptible during flight above the flutter speed. The bandwidth of the actuator is approximately 6.5 Hz which provides predictable gain and phase at the 2.4 Hz flutter mode frequency.

Control of each CCV system is accomplished through panels located at the pilot's and flight engineer's stations. A picture of the pilot's engage panel is presented in Fig. 10. The flight engineer's panel is similar. To engage a system the flight engineer determines that the mode is functional and depresses the associated system switch. When the pilot depresses his corresponding mode switch, the system becomes operative. Only the pilot can engage a system, but both he and the flight engineer can disengage a system.

Table 2 Dimensions of aileron and flaperon control surfaces

	Chord (in.)	Span (in.)
outboard aileron	25	101.5
outboard flaperon	35	95

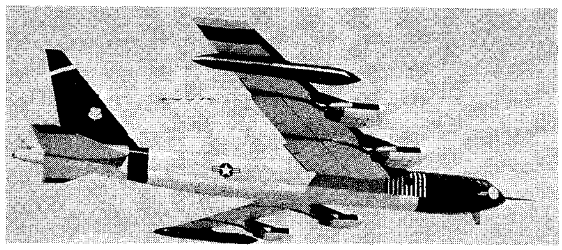

Fig. 9 Modified test airplane.

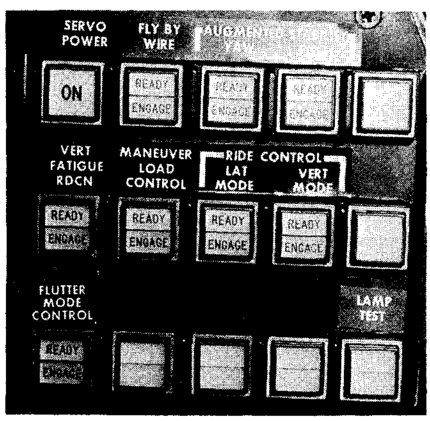

Fig. 10 Pilots engage panel.

System Ground Tests

Prior to beginning the series of flight tests, an extensive ground test of the FMC implementation was accomplished to assure airplane and system flightworthiness. A block diagram showing the mechanization of these ground tests is presented in Fig. 11. Special test inputs are introduced from: 1) the on-board signal generator to determine hysteresis and step response; 2) the transfer function analyzer to determine frequency response; and 3) the flight engineer's test panel to confirm correct system operation during preflight checks. Test inputs may also be introduced from the FBW pilot's controls. Responses to test inputs are recorded on an $X-Y$ plotter, or the on-board oscillograph, from on-board digital voltmeter readings or the transfer function analyzer. A matrix is presented in Fig. 12 that shows the different types of component and system tests conducted.

The L.H. outboard aileron actuator frequency response shown in Fig. 13 is typical of ground test results for both wing actuators. All actuators were implemented with a piston bypass orifice to provide damping and a notch filter in the forward path of the actuator loop to achieve the required closed loop response. The orifice was sized to provide a minimum damping (g) of 0.10. The notch filter does not augment damping but decouples the actuator-surface mode from airframe structural modes by reducing the response amplitude. As shown, both of these methods of compensation are required to meet the allowable tolerances.

The measured actuator surface resonance was 23.5 Hz compared to a predicted frequency of 31 Hz. The predicted resonant amplitude was +6 db compared to the measured amplitude of +75. db. The flaperons were tested in a similar manner and showed similar agreement with analytical predictions. Prior to each flight the FMC system was functionally tested as a part of the routine preflight tests using end-to-end step responses.

Flutter Test Results

During flutter testing, the existence of the baseline (systems off) airplane flutter mode was verified. The flutter speeds for both the 260,000 lb and 375,000 lb configuration were about 7% higher than predicted, as shown in Fig. 14.

The FMC performance was satisfactory and the test objective of flying 10 knots past flutter was met or exceeded for both gross weights. The speed-damping (V-g) plots for these flights are shown in Figs. 15a and 15b. The airplane remained above the FMC-off flutter speed approximately 4 min for each configuration, while the pilot performed normal flutter testing.

Addition of the Maneuver Load Control, Ride Control, and Fatigue Reduction Systems further increased the damping of the lowest damped wing mode as shown in Fig. 16. No CCV system or combination of systems caused a reduction of the flutter speed below that of the basic airplane.

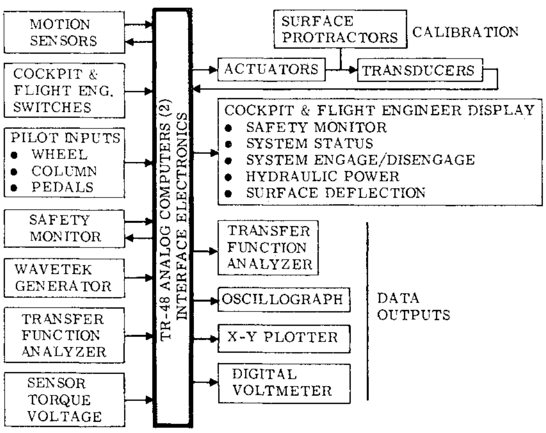

Fig. 11 Ground test mechanization.

TESTS	ACTUATORS – PILOT – ELEVATOR	ACTUATORS – PILOT – RUDDER	ACTUATORS – PILOT – PARALLEL SERVO	ACTUATORS – PILOT – AILERON	ACTUATORS – PILOT – SPOILER	ACTUATORS – FMC – AILERON	ACTUATORS – FMC – FLAPERON	SENSORS – ACCELEROMETERS	FBW CONTROL – COLUMN	FBW CONTROL – WHEEL	FBW CONTROL – PEDAL	FMC ELEMENTS – ELECTRONICS	FMC ELEMENTS – END-TO-END SENSOR, ELECTRONICS AND ACTUATOR
FREQUENCY RESPONSE	X	X	X	X		X	X	X				X	X
CALIBRATION, SCALING AND PHASING	X	X	X	X	X	X	X	X	X	X	X	X	
HYSTERESIS	X	X	X	X	X	X	X	X	X	X	X		
STEP RESPONSE						X	X						X

Fig. 12 System ground test matrix.

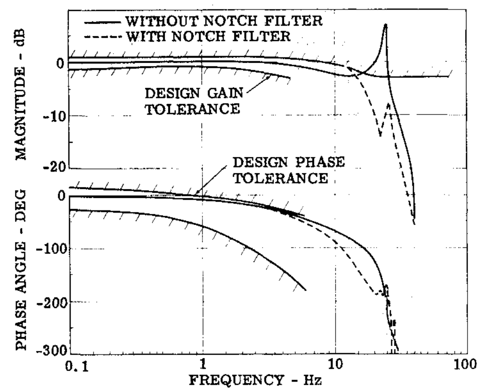

Fig. 13 Outboard aileron ground test frequency response.

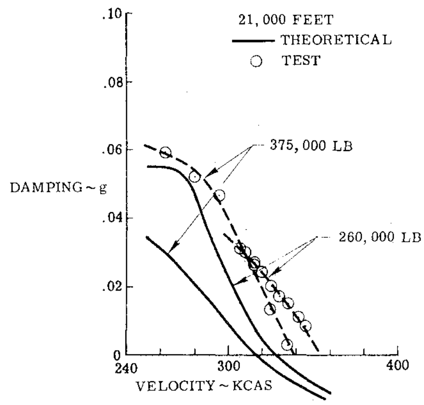

Fig. 14 Test and predicted V-g, FMC off.

Test telemetered and predicted transient responses 10 knots below flutter for a typical pilot flutter test elevator input are shown in Fig. 17. The predicted response was obtained by inverse Laplace transform using a 24-mode set of equations of motion, and includes the telemetry ground station double integration and filtering. The slow beating of the wing tip response which might otherwise have been alarming during test, was predicted accurately. Test transient responses two knots below FMC-off flutter are shown in Fig. 18, both with and without FMC. Without FMC, the flutter mode was essentially neutrally stable.

The transient responses of the FMC control surfaces, the pilot test input, and the cockpit vertical acceleration are shown in Fig. 19, flying 12 knots above the (FMC-off) flutter speed with FMC engaged. The pilot input was sufficiently strong to cause vertical accelerations at the cockpit in excess of 1g incremental. The flaperon required a peak deflection of only four degrees and the outboard aileron only 3°. The pilots reported the FMC system made the airplane response typical of the most stable B-52 configurations.

Conclusions

The flight demonstration of active flutter suppression was completed successfully. The analytical methods used to predict the flutter, the controllability of flutter, and the hardware performance were, when used with the specified design criteria and tolerances, adequate for the task. The hardware performance was predictable analytically to frequencies much higher than required for this test.

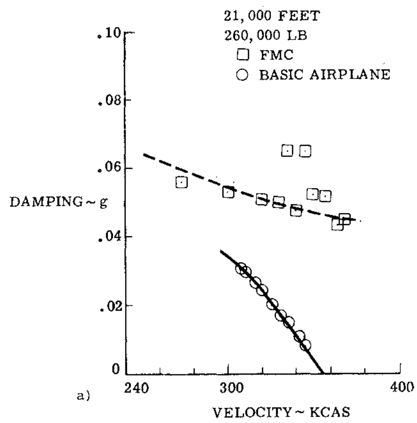

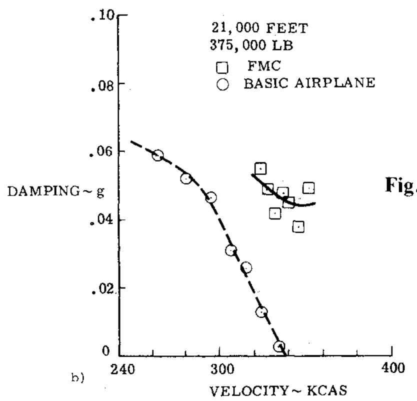

Fig. 15 Test V-g, FMC on.

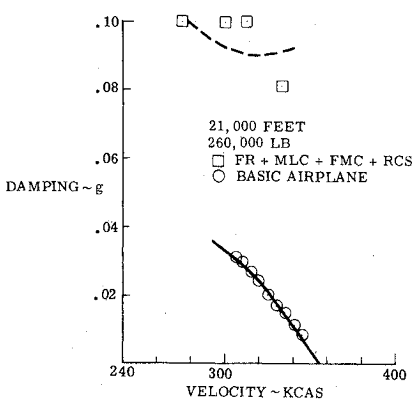

Fig. 16 Test V-g, FMC, MLC, RC, RF, on.

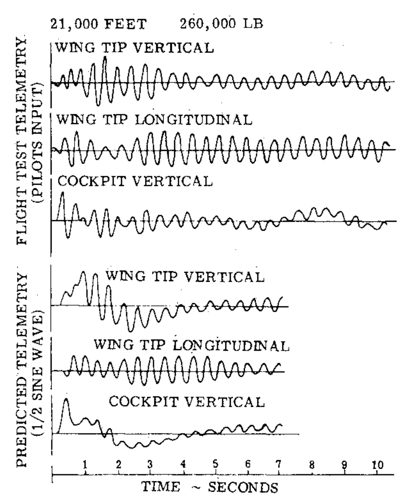

Fig. 17 Test and predicted transient response, 10 knots below flutter.

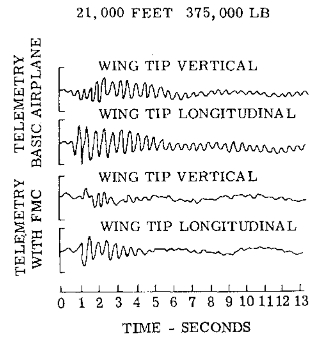

Fig. 18 Test transient response, 2 knots below flutter, with and without FMC.

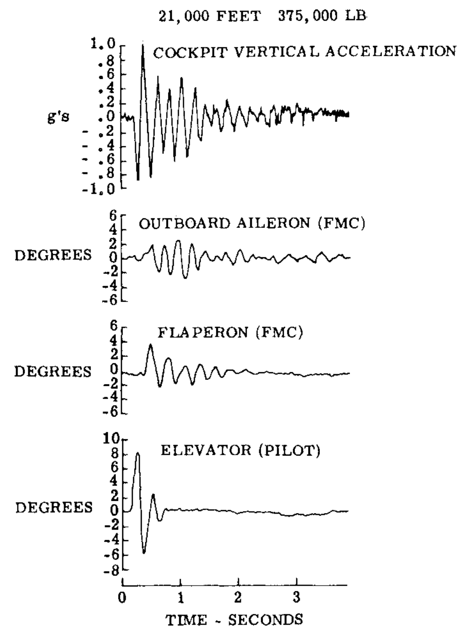

Fig. 19 FMC transient response, 12 knots above flutter.

The authors' opinion was strengthened, on the basis of these tests, that whenever structural and aerodynamic theory are adequate to predict flutter, the controllability of flutter is also predictable. Whether FMC is applicable to more violent, higher frequency modes can then be decided analytically for each specific airplane. For those cases where wind tunnel testing is necessary to determine flutter, tunnel testing of the active FMC system will be equally necessary—parameter identification methods will need to be developed to support experimental control synthesis.

These flights have demonstrated that the benefits and penalties, mechanization and operation of active flutter control systems are within the scope of current engineering analytical methods. The successful conclusion of a flight flutter test program is to report that nothing very surprising happened.

References

[1] Johannes, R. P. and Thompson, G. O., "B-52 Control Configured Vehicles Program," AGARD-CCP-137, Geilo, Norway, Sept. 1973.

[2] Hodges, G. E., "Active Flutter Suppression—B-52 Controls Configured Vehicle," AIAA Paper 73-322, Williamsburg, Va., 1973.

[3] Burris, P. M. and Bender, M. A., "Aircraft Load Alleviation and Mode Stabilization (LAMS) Flight Demonstration Test Analysis," AFFDL-TR-68-164, Dec. 1960, Air Force Flight Dynamics Lab., Wright-Patterson Air Force Base, Ohio.

[4] Stockdale, C. R. and Poyneer, R. D., "Control Configured Vehicle Ride Control System, B-52 Control System Analysis, Synthesis, and Design," AFFDL-TR-73-83, July 1973, Air force Flight Dynamics Lab., Wright-Patterson Air Force Base, Ohio.

[5] McKenzie, J. R., "B-52 Control Configured Vehicles Ride Control Analysis and Flight Test," AIAA Paper 73-782, St. Louis, Mo., 1973.